Supplementary Materials

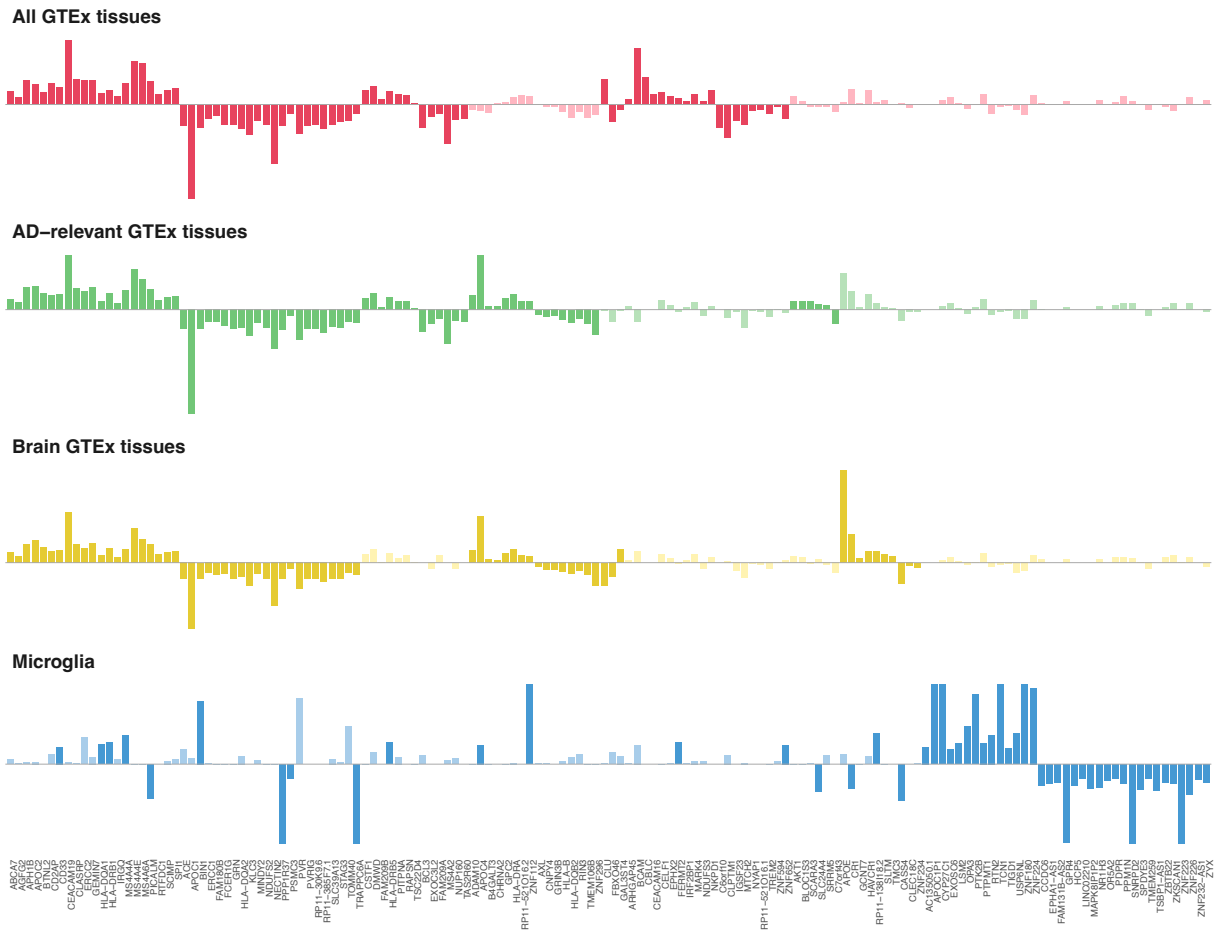

Supplementary Fig. 1. Labeled transcriptomic signatures of AD. Bar plots comparing the four AD gene expression signatures used to query CMap. Genes are labeled on the x-axis and aligned across panels. Bars represent each gene's TWAS *Z*-score for association between genetically predicted expression and AD risk ($Z>0$ indicates higher predicted expression associated with increased AD risk; $Z<0$ indicates higher predicted expression associated with decreased AD risk). Opaque bars denote genes included in the signature submitted to CMap, whereas semi-transparent bars denote genes with TWAS results not included in that signature.

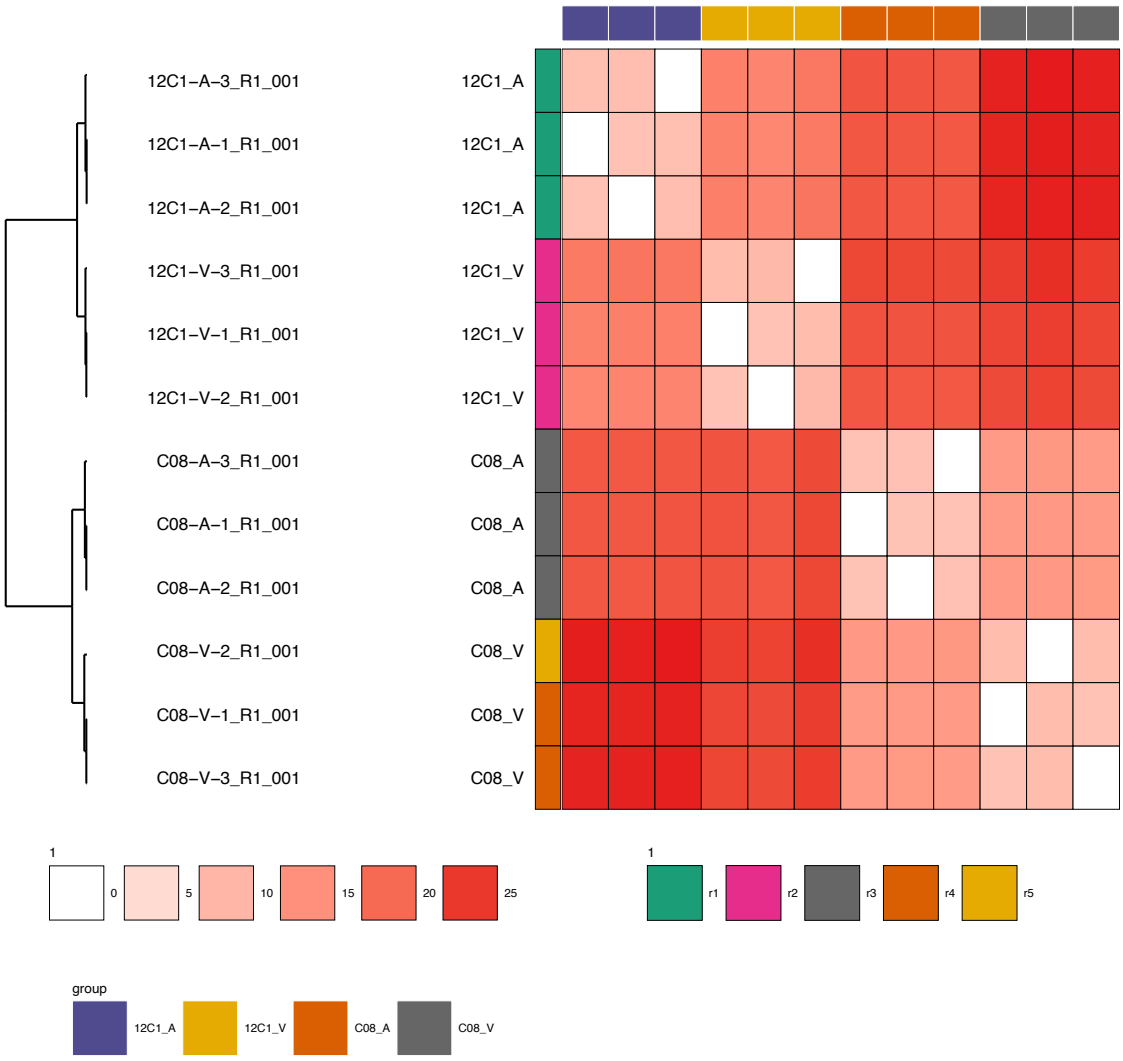

Supplementary Fig. 2. Heatmap of pairwise sample correlations for RNA-seq quality control. Replicates cluster cleanly by their assigned labels, indicating data quality consistent with expectations.

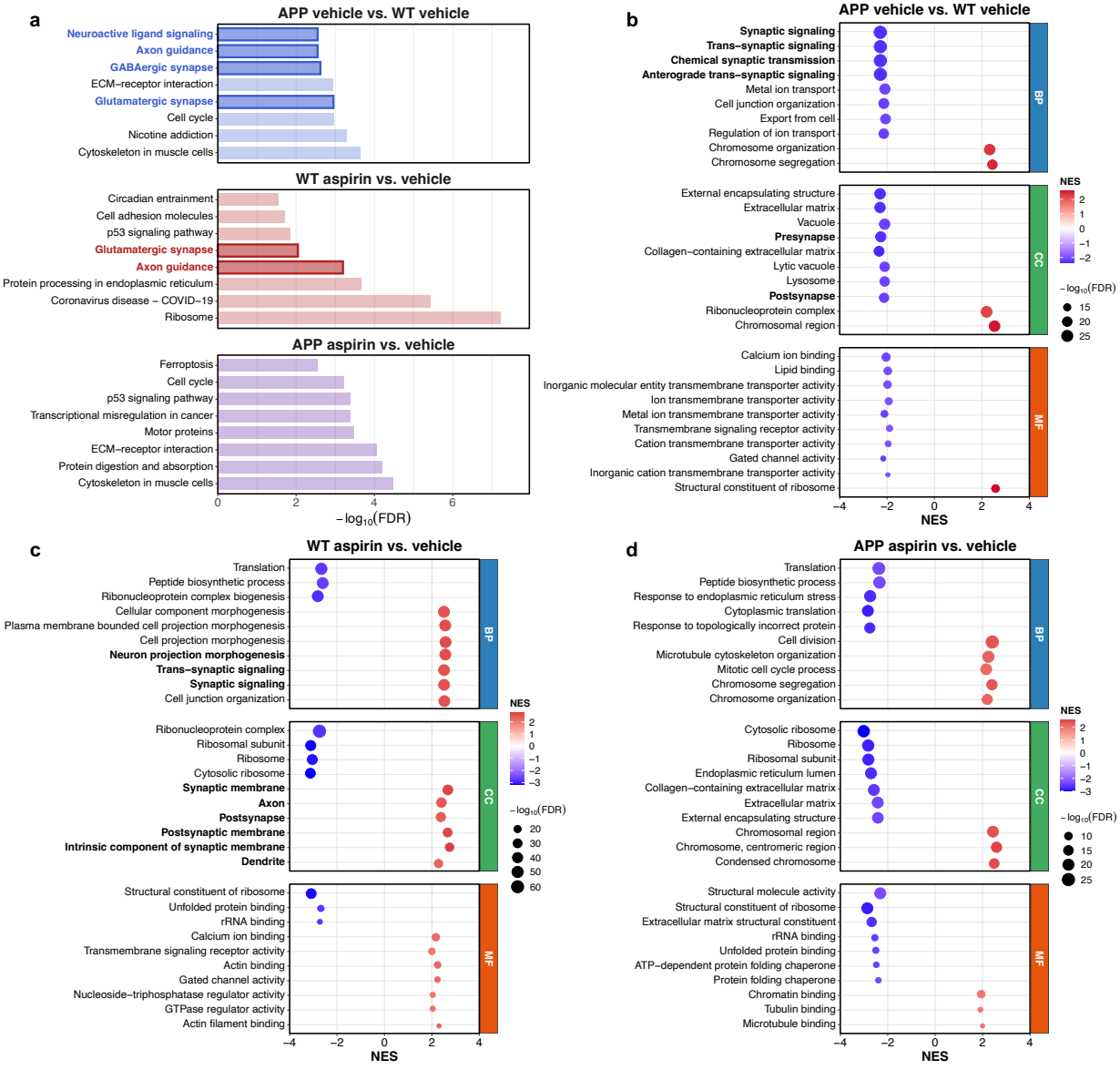
a
APP vehicle vs. WT vehicle
Neuroactive ligand signaling
Axon guidance
GABAergic synapse
ECM–receptor interaction
Glutamatergic synapse
Cell cycle
Nicotine addiction
Cytoskeleton in muscle cells
WT aspirin vs. vehicle
Circadian entrainment
Cell adhesion molecules
p53 signaling pathway
Glutamatergic synapse
Axon guidance
Protein processing in endoplasmic reticulum
Coronavirus disease – COVID–19
Ribosome
APP aspirin vs. vehicle
Ferroptosis
Cell cycle
p53 signaling pathway
Transcriptional misregulation in cancer
Motor proteins
ECM–receptor interaction
Protein digestion and absorption
Cytoskeleton in muscle cells
0
2
4
6
−log10(FDR)
b
APP vehicle vs. WT vehicle
Synaptic signaling
Trans–synaptic signaling
Chemical synaptic transmission
Anterograde trans–synaptic signaling
Metal ion transport
Cell junction organization
Export from cell
Regulation of ion transport
Chromosome organization
Chromosome segregation
BP
External encapsulating structure
Extracellular matrix
Vacuole
Presynapse
Collagen–containing extracellular matrix
Lytic vacuole
Lysosome
Postsynapse
Ribonucleoprotein complex
Chromosomal region
CC
Calcium ion binding
Lipid binding
Inorganic molecular entity transmembrane transporter activity
Ion transmembrane transporter activity
Metal ion transmembrane transporter activity
Transmembrane signaling receptor activity
Cation transmembrane transporter activity
Gated channel activity
Inorganic cation transmembrane transporter activity
Structural constituent of ribosome
MF
−4
−2
0
2
4
NES
NES
2
1
0
−1
−2
−log10(FDR)
15
20
25
c
WT aspirin vs. vehicle
Translation
Peptide biosynthetic process
Ribonucleoprotein complex biogenesis
Cellular component morphogenesis
Plasma membrane bounded cell projection morphogenesis
Cell projection morphogenesis
Neuron projection morphogenesis
Trans–synaptic signaling
Synaptic signaling
Cell junction organization
BP
Ribonucleoprotein complex
Ribosomal subunit
Ribosome
Cytosolic ribosome
Synaptic membrane
Axon
Postsynapse
Postsynaptic membrane
Intrinsic component of synaptic membrane
Dendrite
CC
Structural constituent of ribosome
Unfolded protein binding
rRNA binding
Calcium ion binding
Transmembrane signaling receptor activity
Actin binding
Gated channel activity
Nucleoside–triphosphatase regulator activity
GTPase regulator activity
Actin filament binding
MF
−4
−2
0
2
4
NES
NES
2
1
0
−1
−2
−3
−log10(FDR)
20
30
40
50
60
d
APP aspirin vs. vehicle
Translation
Peptide biosynthetic process
Response to endoplasmic reticulum stress
Cytoplasmic translation
Response to topologically incorrect protein
Cell division
Microtubule cytoskeleton organization
Mitotic cell cycle process
Chromosome segregation
Chromosome organization
BP
Cytosolic ribosome
Ribosome
Ribosomal subunit
Endoplasmic reticulum lumen
Collagen–containing extracellular matrix
Extracellular matrix
External encapsulating structure
Chromosomal region
Chromosome, centromeric region
Condensed chromosome
CC
Structural molecule activity
Structural constituent of ribosome
Extracellular matrix structural constituent
rRNA binding
Unfolded protein binding
ATP–dependent protein folding chaperone
Protein folding chaperone
Chromatin binding
Tubulin binding
Microtubule binding
MF
−4
−2
0
2
4
NES
NES
2
1
0
−1
−2
−3
−log10(FDR)
10
15
20
25

Supplementary Fig. 3. KEGG and Gene Ontology (GO) enrichment analyses. a) KEGG over-representation analysis of differentially expressed genes for three contrasts: baseline APP mutation signature (APP vehicle vs. WT vehicle), aspirin effect in WT (WT aspirin vs. vehicle), and aspirin effect in APP (APP aspirin vs. vehicle). Bar length indicates significance as $-\log_{10}$ false discovery rate (FDR). Synapse, axon, and neuronal signaling pathways are bolded and outlined. **b-d)** GO gene set enrichment analysis (GSEA) for the same three contrasts, showing the top ten enriched terms within biological process (BP), cellular component (CC), and molecular function (MF). The x-axis shows normalized enrichment score (NES). Bubble size is proportional to $-\log_{10}$(FDR); bubble color reflects NES (red, positive; blue, negative).

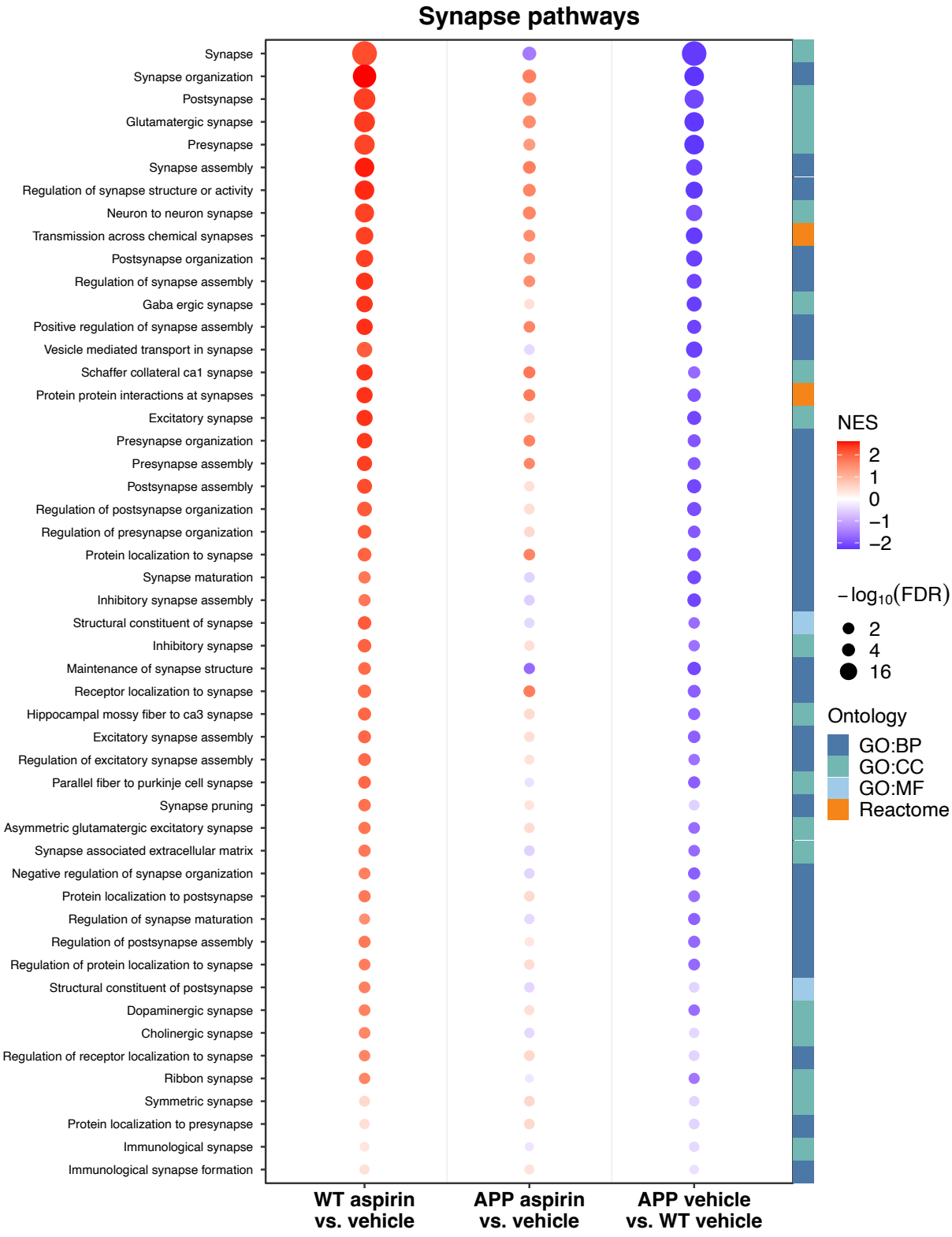
Synapse pathways
Synapse
Synapse organization
Postsynapse
Glutamatergic synapse
Presynapse
Synapse assembly
Regulation of synapse structure or activity
Neuron to neuron synapse
Transmission across chemical synapses
Postsynapse organization
Regulation of synapse assembly
Gaba ergic synapse
Positive regulation of synapse assembly
Vesicle mediated transport in synapse
Schaffer collateral ca1 synapse
Protein protein interactions at synapses
Excitatory synapse
Presynapse organization
Presynapse assembly
Postsynapse assembly
Regulation of postsynapse organization
Regulation of presynapse organization
Protein localization to synapse
Synapse maturation
Inhibitory synapse assembly
Structural constituent of synapse
Inhibitory synapse
Maintenance of synapse structure
Receptor localization to synapse
Hippocampal mossy fiber to ca3 synapse
Excitatory synapse assembly
Regulation of excitatory synapse assembly
Parallel fiber to purkinje cell synapse
Synapse pruning
Asymmetric glutamatergic excitatory synapse
Synapse associated extracellular matrix
Negative regulation of synapse organization
Protein localization to postsynapse
Regulation of synapse maturation
Regulation of postsynapse assembly
Regulation of protein localization to synapse
Structural constituent of postsynapse
Dopaminergic synapse
Cholinergic synapse
Regulation of receptor localization to synapse
Ribbon synapse
Symmetric synapse
Protein localization to presynapse
Immunological synapse
Immunological synapse formation
WT aspirin vs. vehicle
APP aspirin vs. vehicle
APP vehicle vs. WT vehicle
NES
2
1
0
−1
−2
−log10(FDR)
2
4
16
Ontology
GO:BP
GO:CC
GO:MF
Reactome

Supplementary Fig. 4. Synapse-related pathway enrichment. Bubble plots show GSEA results for synapse-related MSigDB gene sets across WT aspirin vs. vehicle, APP aspirin vs. vehicle, and APP vehicle vs. WT vehicle contrasts. Bubbles are colored by normalized enrichment score (NES; red indicates positive enrichment, blue indicates negative enrichment) and bubble size denotes statistical significance ($-\log_{10}$FDR). Pathways with FDR<0.05 are shown with opaque bubbles; pathways with FDR≥0.05 are shown with transparent bubbles.


Axon pathways
Axon development
Axon
Distal axon
Regulation of axonogenesis
Axon extension
Main axon
Axon guidance
Central nervous system neuron axonogenesis
Regulation of axon extension
Axon initial segment
Axonal fasciculation
Central nervous system projection neuron axonogenesis
Positive regulation of axonogenesis
Negative regulation of axonogenesis
Axon ensheathment in central nervous system
Response to axon injury
Positive regulation of axon extension
Motor neuron axon guidance
Axoneme assembly
Axonal transport
Regulation of commissural axon pathfinding by slit and robo
Axon cytoplasm
Peripheral axonal degeneration
Retrograde axonal transport
Commissural neuron axon guidance
Regulation of axon extension involved in axon guidance
Juxtaparanode region of axon
Regulation of axon guidance
Axon guidance receptor activity
Negative regulation of axon extension
Axonal transport of mitochondrion
Axonemal microtubule
Sperm axoneme assembly
Retinal ganglion cell axon guidance
Anterograde axonal transport
Axonemal dynein complex assembly
Axonal growth cone
Peripheral nervous system axon ensheathment
Protein localization to axon
Mixed demyelinating and axonal polyneuropathy
Axonemal doublet microtubule
Sema3a pak dependent axon repulsion
Axonal degeneration
Axonemal a tubule inner sheath
Dynein axonemal particle
Axonemal dynein complex
Axonal loss
Emg axonal abnormality
Sensory axonal neuropathy
Motor axonal neuropathy
Axonogenesis involved in innervation
WT aspirin vs. vehicle
APP aspirin vs. vehicle
APP vehicle vs. WT vehicle
NES
2
1
0
−1
−2
−log10(FDR)
2
4
16
Ontology
GO:BP
GO:CC
GO:MF
HPO
Reactome
WikiPathways

Supplementary Fig. 5. Axon-related pathway enrichment. Bubble plots show GSEA results for axon-related MSigDB gene sets across WT aspirin vs. vehicle, APP aspirin vs. vehicle, and APP vehicle vs. WT vehicle contrasts. Bubbles are colored by normalized enrichment score (NES; red indicates positive enrichment, blue indicates negative enrichment) and bubble size denotes statistical significance ($-\log_{10}$FDR). Pathways with FDR<0.05 are shown with opaque bubbles; pathways with FDR≥0.05 are shown with transparent bubbles.

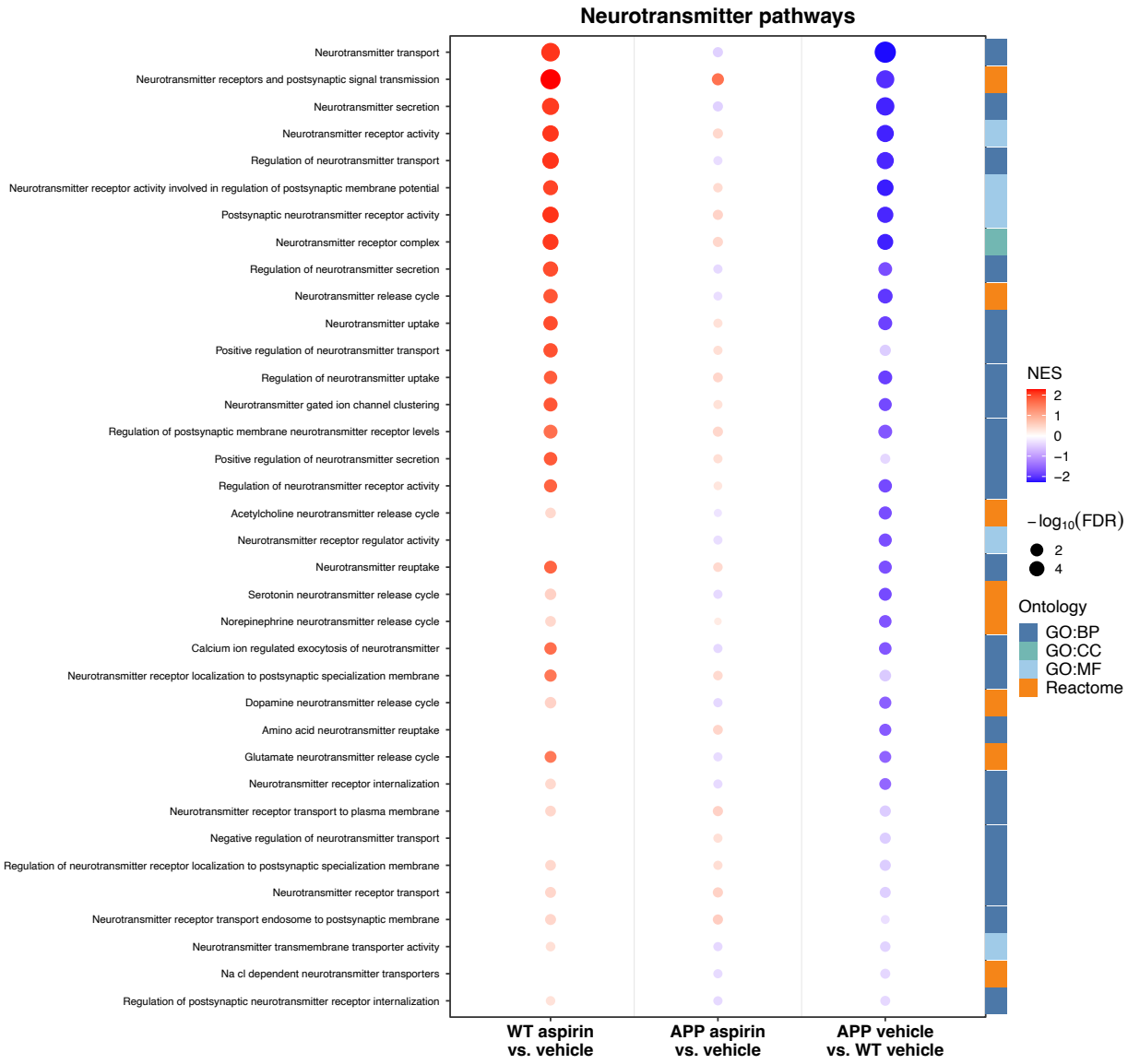

Supplementary Fig. 6. Neurotransmitter-related pathway enrichment. Bubble plots show GSEA results for neurotransmitter-related MSigDB gene sets across WT aspirin vs. vehicle, APP aspirin vs. vehicle, and APP vehicle vs. WT vehicle contrasts. Bubbles are colored by normalized enrichment score (NES; red indicates positive enrichment, blue indicates negative enrichment) and bubble size denotes statistical significance ($-\log_{10}$FDR). Pathways with FDR<0.05 are shown with opaque bubbles; pathways with FDR≥0.05 are shown with transparent bubbles.

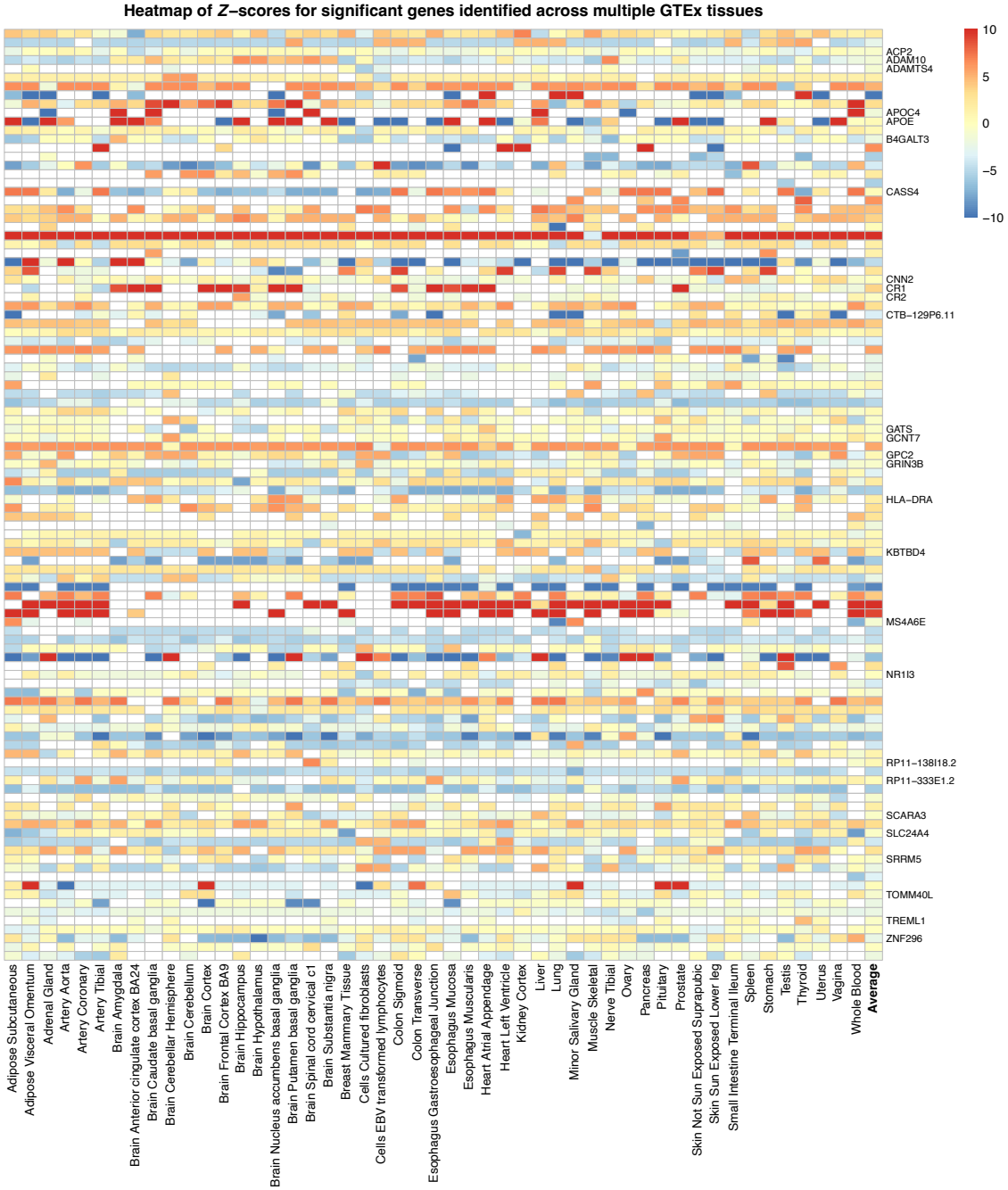
Heatmap of Z−scores for significant genes identified across multiple GTEx tissues
10
5
0
−5
−10
ACP2
ADAM10
ADAMTS4
APOC4
APOE
B4GALT3
CASS4
CNN2
CR1
CR2
CTB−129P6.11
GATS
GCNT7
GPC2
GRIN3B
HLA−DRA
KBTBD4
MS4A6E
NR1I3
RP11−138I18.2
RP11−333E1.2
SCARA3
SLC24A4
SRRM5
TOMM40L
TREML1
ZNF296
Adipose Subcutaneous
Adipose Visceral Omentum
Adrenal Gland
Artery Aorta
Artery Coronary
Artery Tibial
Brain Amygdala
Brain Anterior cingulate cortex BA24
Brain Caudate basal ganglia
Brain Cerebellar Hemisphere
Brain Cerebellum
Brain Cortex
Brain Frontal Cortex BA9
Brain Hippocampus
Brain Hypothalamus
Brain Nucleus accumbens basal ganglia
Brain Putamen basal ganglia
Brain Spinal cord cervical c1
Brain Substantia nigra
Breast Mammary Tissue
Cells Cultured fibroblasts
Cells EBV transformed lymphocytes
Colon Sigmoid
Colon Transverse
Esophagus Gastroesophageal Junction
Esophagus Mucosa
Esophagus Muscularis
Heart Atrial Appendage
Heart Left Ventricle
Kidney Cortex
Liver
Lung
Minor Salivary Gland
Muscle Skeletal
Nerve Tibial
Ovary
Pancreas
Pituitary
Prostate
Skin Not Sun Exposed Suprapubic
Skin Sun Exposed Lower leg
Small Intestine Terminal Ileum
Spleen
Stomach
Testis
Thyroid
Uterus
Vagina
Whole Blood
Average

Supplementary Fig. 7. Tissue-specific S-PrediXcan results. Heatmap of S-PrediXcan *Z*-scores across GTEx tissues for genes significant in more than one tissue. Rows indicate genes and columns indicate tissues. Color denotes *Z*-score magnitude and direction ($Z>0$: higher genetically predicted expression associated with increased AD risk; $Z<0$: higher genetically predicted expression associated with decreased AD risk). The rightmost "Average" column reports each gene's mean *Z*-score across tissues with non-missing estimates.

Supplementary Table 1. AD-associated genes represented in TWAS-derived transcriptomic signatures and supporting evidence.

Gene	Evidence type	References
ABCA7	GWAS locus	1,2
CD2AP	GWAS locus, TWAS risk gene	1–5
CD33	GWAS locus; TWAS risk gene	1–3,6
HLA-DQA1†	GWAS locus	7
HLA-DRB1†	GWAS locus	1,2
MS4A4A	GWAS locus; TWAS risk gene	3,6,8
MS4A6A	GWAS locus; TWAS risk gene	1,2,6
PICALM	GWAS locus; TWAS risk gene	1–4,6,9
ACE	TWAS risk gene	4,10
APOC1	TWAS risk gene	5
BIN1	GWAS locus; TWAS risk gene	1–3,6,8,9
HLA-DQA2†	TWAS risk gene	11
PVR	TWAS risk gene	6,8,11
TOMM40	TWAS risk gene	6,11,12
DMWD	TWAS risk gene	6,11
HLA-DRB5†	GWAS locus	1
ADAM10	GWAS locus	2
HLA-DRA†	Gene-based GWAS association	2
HLA-DQB2†	Candidate risk gene at GWAS locus	1,13
CLU	GWAS locus; TWAS risk gene	1–3,6
IRF2BP1	TWAS risk gene	11
CLPTM1	TWAS risk gene	6,11
TREM2	GWAS locus; TWAS risk gene	2,5
APOE	GWAS locus; TWAS risk gene	1,2,8,9,11
CR1	GWAS locus; TWAS risk gene	1–3,6,11
PTK2B	GWAS locus; TWAS risk gene	1,2,6,8

† Due to high linkage disequilibrium in the HLA region, locus-level associations cannot reliably be resolved to a single causal gene.

Supplementary Table 2. Characteristics of matched patient cohort for MarketScan claims data case-control study.

Clinical characteristics	**MarketScan** (*N* = 248,961)	
AD status	**Case (AD)**	**Control (no AD)**
N	82,987	165,974
Mean age at last follow-up (s.d.)	85.6 (7.1)	84.2 (7.2)
Sex (%)		
Female	65.1	65.1
Male	34.9	34.9
Comorbidities (%)		
Cardiovascular disease	52.1	46.6
Cerebrovascular disease	35.9	26.7
Rheumatoid arthritis	3.4	3.9

Supplementary Table 3. AD outcomes in VUMC, *All of Us*, and MarketScan datasets.

Clinical characteristics	**VUMC** (*N* = 19,413)		***All of Us*** (*N* = 1,995)		**MarketScan** (*N* = 248,961)	
Aspirin	**Exposed**	**Unexposed**	**Exposed**	**Unexposed**	**Exposed**	**Unexposed**
AD diagnoses (*N*)	152	387	–	–	196	82,791
Mean age of AD diagnosis among AD cases (s.d.)	76.1 (3.9)	76.7 (4.0)	76.0 (2.2)	76.8 (2.7)	85.6 (7.2)	84.2 (7.2)

*Participant counts for the NIH *All of Us* Research Program data are not reported if between 1 and 20, in compliance with data privacy and reporting restrictions set by *All of Us*.

Supplementary References

1. Lambert, J.-C. *et al.* Meta-analysis of 74,046 individuals identifies 11 new susceptibility loci for Alzheimer's disease. *Nat Genet* **45**, 1452–1458 (2013).
2. Jansen, I. E. *et al.* Genome-wide meta-analysis identifies new loci and functional pathways influencing Alzheimer's disease risk. *Nat Genet* **51**, 404–413 (2019).
3. Naj, A. C. *et al.* Common variants at MS4A4/MS4A6E, CD2AP, CD33 and EPHA1 are associated with late-onset Alzheimer's disease. *Nat Genet* **43**, 436–441 (2011).
4. Sun, Y. *et al.* A transcriptome-wide association study identifies novel blood-based gene biomarker candidates for Alzheimer's disease risk. *Hum Mol Genet* **31**, 289–299 (2021).
5. Gockley, J. *et al.* Multi-tissue neocortical transcriptome-wide association study implicates 8 genes across 6 genomic loci in Alzheimer's disease. *Genome Med* **13**, 76 (2021).
6. Hao, S., Wang, R., Zhang, Y. & Zhan, H. Prediction of Alzheimer's Disease-Associated Genes by Integration of GWAS Summary Data and Expression Data. *Front Genet* **9**, 653 (2019).
7. Bellenguez, C. *et al.* New insights into the genetic etiology of Alzheimer's disease and related dementias. *Nat Genet* **54**, 412–436 (2022).
8. Harwood, J. C. *et al.* Defining functional variants associated with Alzheimer's disease in the induced immune response. *Brain Commun* **3**, fcab083 (2021).
9. Sun, N. *et al.* Human microglial state dynamics in Alzheimer's disease progression. *Cell* **186**, 4386-4403.e29 (2023).
10. Sun, Y. *et al.* A transcriptome-wide association study of Alzheimer's disease using prediction models of relevant tissues identifies novel candidate susceptibility genes. *Genome Med* **13**, 141 (2021).

11. Gerring, Z. F., Lupton, M. K., Edey, D., Gamazon, E. R. & Derks, E. M. An analysis of genetically regulated gene expression across multiple tissues implicates novel gene candidates in Alzheimer's disease. *Alzheimer's Research & Therapy* **12**, 43 (2020).
12. Tang, S. *et al.* Novel Variance-Component TWAS method for studying complex human diseases with applications to Alzheimer's dementia. *PLOS Genetics* **17**, e1009482 (2021).
13. Zhang, X. *et al.* Regulation of the Late Onset alzheimer's Disease Associated HLA-DQA1/DRB1 Expression. *Am J Alzheimers Dis Other Demen* **37**, 15333175221085066 (2022).